

# Thermal-Expansion and Fracture Toughness Properties of Parts made from Liquid Crystal Stereolithography Resins

J. S. Ullett, T. Benson-Tolle\*, J. W. Schultz\*\* and R. P. Chartoff

The Rapid Prototype Development Laboratory and  
Ohio Rapid Prototype Process Development Consortium, Dayton, OH 45469-0130

\*The WL/MLBC, Wright-Patterson AFB 45433-7750

\*\*The Georgia Tech Research Institute, Atlanta, GA 30332-0824

## Introduction

Liquid crystal (LC) resins are a new kind of stereolithography material that can produce parts with structured or ordered morphologies instead of the amorphous morphologies that result from standard resins. The LC molecules can be aligned before cure resulting in an anisotropic crosslinked network when the laser induced polymerization “locks-in” the alignment. Previous papers have explored liquid crystal orientation dynamics [1], the effects of orientation on visco-elastic and mechanical properties [2,3], and the processing of LC resins by stereolithography [4]. This paper considers the effects of morphology on fracture toughness and thermal-expansion properties. Both toughness and thermal-stability continue to be important issues for stereolithography parts. The use of LC resins may provide a way to significantly improve performance in both of these areas, and in addition result in parts with high upper use temperatures.

## Background

### *The Role of Morphology in Fracture Toughness*

The importance of morphology and microstructure on material properties has been long recognized by materials scientists. In metals, goals of increased strength and toughness have been addressed through improving alloy chemistry or increasing purity; developing and optimizing microstructures and phase distributions; and manipulating microstructures. Manipulation of microstructures through processing often has the objective of obtaining microstructural anisotropy for some improved mechanical property.

Orientation of polymeric molecules to increase strength and stiffness has been practiced by the fiber industry and been achieved through techniques such as drawing, spinning or extruding. Pitch-based fibers employ orientation and anisotropy of morphology as well. Though pitch was used as a carbon fiber precursor and spun into filaments in 1965, the breakthrough which provided high properties came in 1973 when pitch was first transformed from an amorphous material into a liquid crystalline (mesophase) state prior to spinning into a filament. The LC pitch is then sent through a spinning and extruding operation which orders and aligns the polymer prior to it being stabilized, carbonized and graphitized. This alignment of the morphology and molecular bonds results in anisotropic properties with higher properties in the aligned direction.

Fracture toughness is a mechanical property of importance to many applications. Fracture toughness is defined as a material's resistance to brittle fracture. The fracture toughness of a material is very sensitive to morphology, anisotropy and planes of weakness [5]. A material's morphology can provide mechanisms that enhance energy absorption during fracture and hence enhance fracture toughness. Such mechanisms include those that shield the crack tip

from the full extent of the driving force, deflect the crack path, pin the crack front, shield the tip and creating a favorable residual stress pattern, or relax the crack tip stress. Microstructural alignment through processing or morphology can play a large role in such mechanisms.

Highly crosslinked thermosets typically fracture in a brittle manner at conventional test rates. The concepts of linear elastic fracture mechanics (LEFM) have been successfully applied to such materials as epoxies, acrylates, unsaturated polyesters, and vinyl ester resins. In this research, ordered (non-aligned) nematic and isotropic LC thermosets were fabricated by stereolithography and fracture toughness testing was performed with the objective of determining the effect of the liquid-crystal phase on fracture toughness.

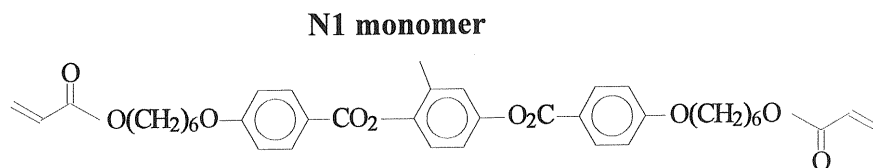
#### *The Effect of Alignment on Thermal-Expansion Properties*

The effect of molecular alignment on thermal expansion has been well studied in polymeric materials, in particular, fibers. The effects of alignment in liquid crystal thermosets has also been studied. Broer and Mol [6] studied the anisotropic thermal expansion of a series of LC thermosets. They found that as the order parameter increased with change in spacer length, the anisotropy in the linear thermal expansion increased as well. They observed a greater difference above the glass transition temperature than below it.

Thermal expansion measurements of aligned films provide benchmark values to which thermal expansion of multi-layered parts can be compared. The usual process by which films are made allows for more perfect alignment compared with the stereolithography process. The modified LC stereolithography process [7] provides the flexibility to change alignment directions from one layer to the next. This is akin to altering the fiber direction in continuous fiber reinforced composites (FRC). Properties of multi-layer LC structures that are unidirectionally aligned can be compared with the properties of aligned films to assess the overall alignment in the structures. When the layer-to-layer alignment is varied, as is done in FRCs, the in-plane thermal expansion coefficients can be minimized.

#### **Specimen Fabrication**

Multi-layer specimens for fracture toughness and thermal expansion measurements were made with the table-top stereolithography apparatus (TTSLA) using an Argon ion laser tuned to 364 nm. The laser power level was 35 mW and the beam spot size was about 200 microns. The N1 resin shown below was used for all specimens and was catalyzed with 0.5 % Irgacure 369 photo-initiator from Ciba. The N1 resin temperature was controlled at 85 °C during part build for liquid crystal parts, and 118°C for isotropic parts.



A magnet was used for alignment of the liquid crystal resin. It was mounted on a turntable so its position relative to the build platform could be manually adjusted. A T-square was used to adjust the magnet poles to be either parallel or perpendicular to the build platform. A

four minute wait period was allowed between the time the magnet was positioned and the next layer was drawn. All parts were made using an alternating draw style with a center-to-center spacing of 6 mils (0.152 mm). The layer thickness used was either 10 mils (0.254 mm) or 8 mils (0.203) depending on the part. All parts made were rectangular in shape with the short side measuring about 10 to 15 mm and the long side measuring about 25 to 30 mm.

When the magnetic field was aligned parallel to the long direction of the part the orientation was labeled 0 degrees. Likewise, when the magnetic field was aligned perpendicular to the long direction of the part, the orientation was labeled 90 degrees. Aligned parts were made for thermal expansion studies. Future work will involve fracture toughness analysis of aligned parts. The fracture toughness parts were made either in the un-aligned nematic state or in the isotropic state.

After building a part, it was removed from the platform. Any support structures attached to the part were removed before post-cure. The parts, heated to 150 °C, were post-cured using a broad-band Mercury vapor lamp. The parts were post-cured bottom-side up for two hours; and then top-side up for two hours. Thermal expansion measurements were done using a TA Instruments model 2940 TMA using a scan rate of 5°C/min.

Two draw patterns were tried for building parts in the unaligned nematic phase for fracture toughness testing: the original pattern, and the 3D Systems STARWEAVE [8] style was evaluated with a center-to-center spacing of 8 mils. Parts made from the STARWEAVE pattern were substantially flatter before postcure than parts made with the original style. However, after postcure the STARWEAVE parts were as warped as the original parts. The more open pattern of STARWEAVE leaves more material (particularly below the mid-plane of the part) to be fully cured during the postcure, which causes warpage during postcure. Parts made in the isotropic state were only made using the original draw style.

The parts for fracture toughness testing were cut into compact tension coupons on a diamond cutting wheel, then sanded to obtain plane surfaces and accurate outer dimensions. The dimensions were: length = 0.5 inch, and width = 0.48 inch. Coupon thicknesses varied between 0.10 and 0.15 inch. A drilling jig was utilized with a carbide bit to drill the holes for the compact tension specimen, and a diamond cutting wheel was used to cut the notch. The notch was cut perpendicular to the build layers. The coupons were then polished with a polishing wheel to provide enhanced surface smoothness to better view crack propagation. A starter crack was made by scratching the notch with a sharp razor blade just prior to testing. Specimens were tested using an MTS machine at a crosshead displacement rate of 0.02 inch/minute.

## Results and Discussion

### *Compact Tension Analysis*

Calculations for fracture toughness were made using ASTM Standard E399. This standard is developed for metallic materials and is based on linear elastic fracture mechanics (LEFM), defining the stress intensity factor by assuming a linear elastic material and a state of plane strain. The calculations provide a conditional result  $K_Q$ , the value of the stress intensity factor where a material begins to crack significantly, from the following equation:

$$K_Q = (P_Q/bW^{1/2})*(f(a/W)) \quad (1)$$

where  $P_Q$  = load , lbf, at crack propagation

$b$  = specimen thickness, inches

W = length from the center of the loading hole to the end of the specimen, inches  
a = crack length, inches

and where  $f(a/W)$  is determined from

$$f(a/W) = (2+a/W)\{0.866+4.64a/W-13.32(a/W)^2+14.72(a/W)^3-5.6(a/W)^4\}/(1-a/W)^{3/2} \quad (2)$$

$K_Q$  may equal the plane strain fracture toughness,  $K_{IC}$  (opening mode), if the plastic zone is small compared to the specimen thickness and dimensions, or in other words when a state of plane strain can be assumed. In plane strain, only limited slow-stable crack growth occurs.

Both nematic and isotropic specimens fractured in a stick-slip manner, which is common for thermosets. That is, multiple crack arrest and initiation events occurred before catastrophic failure. The  $a/W$  values closest to 0.5 (value recommended by ASTM E399) are reported for each specimen. Results for the first set of unaligned nematic specimens are given in Table 1. This set was made using the original draw style. The average  $K_Q$  value calculated for seven specimens was 566 psi $\sqrt{\text{in}}$  with a standard deviation of 4.6 % (25 psi $\sqrt{\text{in}}$ ). The results for the second set of unaligned nematic samples are given in Table 2. Recall, these specimens were made using the STARWEAVE drawstyle. The average  $K_Q$  for this specimen set was 639 psi $\sqrt{\text{in}}$  with a standard deviation of 12.7 % (81 psi $\sqrt{\text{in}}$ ). So there was a small (14 %) effect that may be attributable to drawstyle. The overall effect of drawstyle on nematic microstructure is unknown.

**Table 1 Fracture Toughness Results for Unaligned Nematic Samples**

| Specimen #       | a/W   | b, thickness (inch) | $K_Q$ (psi $\sqrt{\text{in}}$ ) |
|------------------|-------|---------------------|---------------------------------|
| 2                | 0.573 | 0.110               | 563                             |
| 3                | 0.500 | 0.092               | 529                             |
| 4                | 0.510 | 0.105               | 550                             |
| 5                | 0.500 | 0.090               | 581                             |
| 6                | 0.537 | 0.085               | 610                             |
| 7                | 0.493 | 0.104               | 572                             |
| 8                | 0.660 | 0.090               | 558                             |
| Avg. (std. dev.) |       |                     | 566 (4.6%)                      |

**Table 2 Fracture Toughness Results for Unaligned Nematic Samples made Using STARWEAVE Drawstyle**

| Specimen #       | a/W   | b, thickness (inch) | $K_Q$ (psi $\sqrt{\text{in}}$ ) |
|------------------|-------|---------------------|---------------------------------|
| a                | 0.533 | 0.100               | 760                             |
| b                | 0.572 | 0.106               | 552                             |
| c                | 0.531 | 0.104               | 623                             |
| d                | 0.51  | 0.085               | 586                             |
| e                | 0.56  | 0.103               | 672                             |
| Avg. (std. dev.) |       |                     | 639 (12.7%)                     |

**Table 3 Fracture Toughness Results for Isotropic Samples**

| Specimen #       | a/W   | b, thickness<br>(inch) | K <sub>Q</sub><br>(psi√in) |
|------------------|-------|------------------------|----------------------------|
| 1                | 0.522 | 0.148                  | 429                        |
| 2                | 0.514 | 0.151                  | 373                        |
| 3                | 0.601 | 0.145                  | 270                        |
| 4                | 0.477 | 0.146                  | 228                        |
| 5                | 0.554 | 0.156                  | 200                        |
| 6                | 0.587 | 0.158                  | 241                        |
| Avg. (std. dev.) |       |                        | 290 (31%)                  |

Results for specimens built in the isotropic state are given in Table 3. The average K<sub>Q</sub> for 6 specimens was 290 psi√in with a standard deviation of 31 % (90 psi√in). The reason for the larger deviation in K<sub>Q</sub> values has not been assigned to a single cause. The lower load values measured for these samples make errors in crack length measurement more of a factor .

Analysis by scanning electron microscopy (SEM) of the nematic and isotropic fracture surfaces suggests an explanation for the higher toughness measured for nematic samples. Figure 1a shows a photomicrograph of a nematic fracture surface. There is considerable surface roughness, which is a qualitative indicator of high toughness. Studies have suggested that the amount of strain energy involved in a fracture may be proportional to the areas of surface created and the amount of plastic deformation at the crack tip [9]. The large number of planes seen on the fracture surface of the nematic specimens indicate that a greater surface area had to be created to move the crack front forward. In contrast, the fracture surface of the isotropic specimens is almost featureless and typical of brittle, glassy materials. It shows only a few river mark patterns perpendicular to the crack front (Figure 1b).

#### *Thermal Expansion of Multi-layered Parts*

Concerning the thermal expansion behavior, the first question to be answered was how do the thermal expansion properties of thick parts manufactured via stereolithography compare with those of thin films made under ideal conditions? Figure 2 shows the thermal expansion of the 16 layer uni-directional N1 part compared with the thermal expansion of N1 films. Table 4 lists linear thermal expansion values above and below the glass transition temperature for these specimens. The transverse, or 90 degree, data matched with no significant difference for the 90 degree film and part. There was a greater difference between the 0 degree film and part. The differences may be due to procedural error in aligning the magnet poles before scanning the film or part, or errors in mounting the film for thermal expansion measurement.

Another possibility is that the differences in the slopes of the expansion curves indicate that the multi-layer part is not as perfectly aligned as the thin film. There are several possible sources of disorder inherent with the laser scanning process. Xu et al. [10] have shown that as a strand of polymer is formed by a scanning laser, considerable flow occurs in the resin surrounding the strand. They attribute the flow to gradients in temperature, and thus density, resulting from released heat of reaction

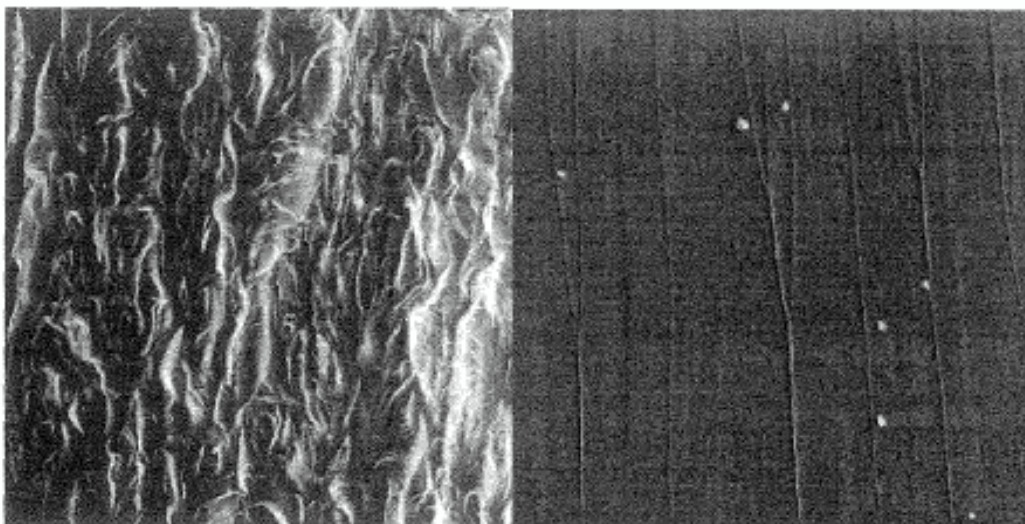
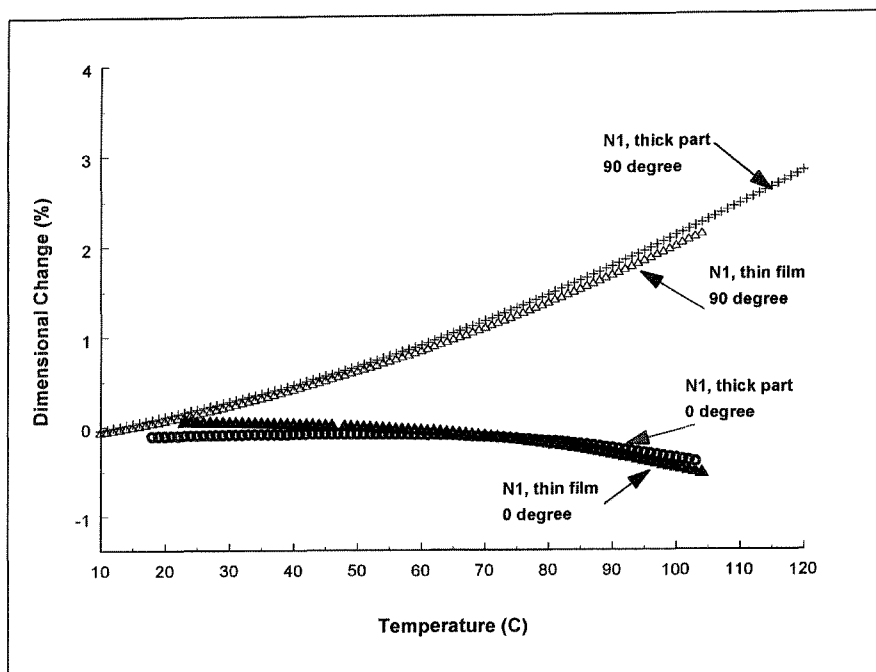


Figure 1: Photomicrographs (250 x) of fracture surfaces from compact tension specimens: a) fracture surface of nematic sample, b) fracture surface of isotropic sample.

The N1 data in Figure 2 indicate that thick parts can be made with a significant degree of alignment resulting in anisotropic thermal expansion properties. A similar anisotropy in thermal expansion properties is characteristic of continuous fiber-reinforced composite plies. In-plane thermal expansion is minimized in composite laminates by arranging the plies at different angles. This technique was evaluated with the aligned N1 resin. A 13 layer part was made having layers aligned alternating between 0 degrees (angle between magnetic field and long side of part) and 90 degrees. The variation in alignment was symmetric about the mid-plane of the part. The first attempt at building this part failed due to delamination at one corner of the part. The 0/90 configuration results in large normal forces at the edges of a part. In the N1 part the normal forces were large enough to cause delamination after about 6 layers were built.

**Table 4 Thermal Expansion Values for N1 Films and Parts**

| N1 Specimen     | $\alpha$ , from 25 to 40 °C | $\alpha$ , from 85 to 100°C |
|-----------------|-----------------------------|-----------------------------|
| Film, 0 degree  | -17.6 ppm/°C                | -139 ppm/°C                 |
| Part, 0 degree  | 7.9 ppm/°C                  | -102 ppm/°C                 |
| Film, 90 degree | 179 ppm/°C                  | 315 ppm/°C                  |
| Part, 90 degree | 180 ppm/°C                  | 328 ppm/°C                  |



Comparison of linear thermal expansion data for N1 thin film and thick part specimens.

To compensate for the normal forces, the layer thickness was decreased from 10 mil to 8 mil keeping the scan speed the same. The result of this change was to generate deeper overcure into the last-built layer. After the part was made, it was removed from the supports and examined. A small (2-3 mm) length of delamination was evident at one corner. This section was cut off using a diamond saw after the part was post-cured. The thermal expansion in the long direction was then measured and compared with the thermal expansion of the uni-directionally aligned 16 layer part as shown in Figure 3. As expected, the thermal expansion of the 0/90 part falls somewhere in between the expansion curves for the 0 degree and the 90 degree part. The in-plane expansion coefficient below the glass transition was about 54 ppm/°C and was about 33 ppm/°C above the glass transition. To eliminate delamination,  $\pm 45$  degree layers need to be used between the 0 degree and 90 degree layers. This type of "lay-up" is commonly used with continuous fiber reinforced composites to minimize normal stresses that can lead to delamination.

## Summary

It has been shown that significant improvements in fracture toughness can be made by processing liquid crystal resins in the un-aligned nematic phase versus the isotropic phase. SEM photomicrographs indicate that considerably greater surface area is formed during the crack propagation process for the unaligned nematic samples. Future work should consider the effects of: layer alignment, alternating alignments layer-to-layer, and alternating alignments strand-to-strand, on fracture toughness.

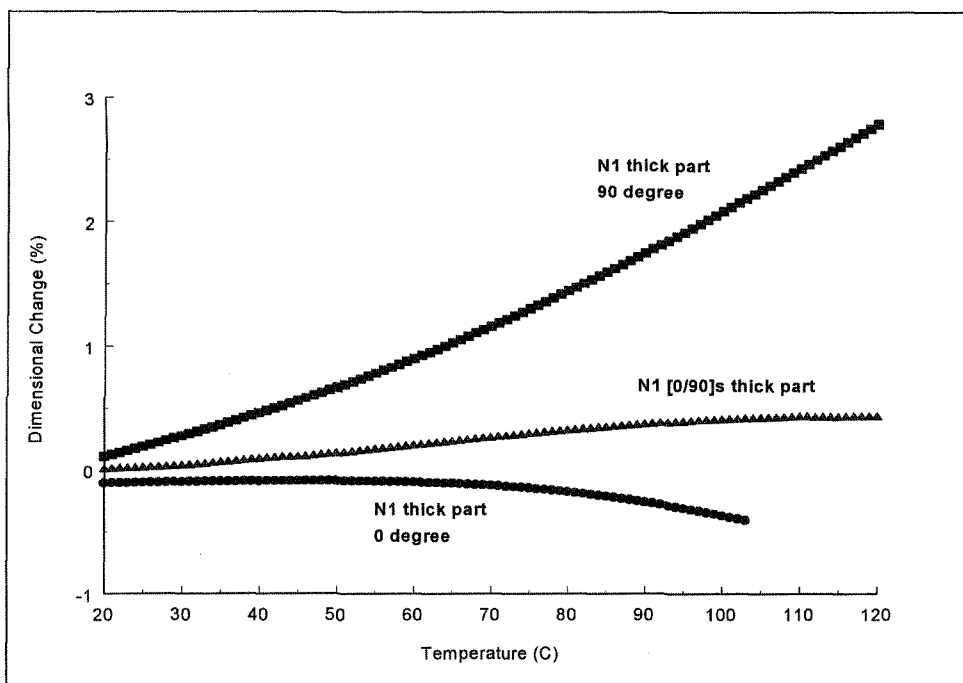


Figure 3. Comparison of N1 thermal expansion data for a 0/90 symmetric part with data for a uni-directionally aligned part.

Thermal expansion measurements of multi-layer parts indicate that considerable alignment of LC monomer can be achieved via a modified LC process. In the direction of alignment the thermal expansion is low below the glass transition temperature and negative above the glass transition temperature.

By alternating the alignment direction layer-to-layer, parts can be made that have low in-plane thermal expansion below and above the glass transition temperature. Consequently, LC resins may be useful in high-temperature applications where in-plane dimensional stability is critical.

### Acknowledgements

The authors are pleased to acknowledge that this research was supported by the U. S. National Science Foundation through NSF Grant # DMR-9420357, from the Polymer Program, Division of Materials Research. Dr. Andrew Lovinger was program manager. From the University of Dayton, we also thank John Murphy for assistance in setting up experiments.

### References

1. J.W. Schultz, R.P. Chartoff, "Photopolymerization of Nematic Liquid Crystal Monomers for Structural Applications: Molecular Order and Orientation Dynamics," (in press) *Polymer* (1998).
2. J.W. Schultz, R.P. Chartoff, J.S. Ullett, "Photopolymerization of Nematic Liquid Crystal Monomers for Structural Applications: Linear Viscoelastic Behavior and Cure Effects," (in press) *Journal of Polymer Science: Part B: Polymer Physics*, (1998).

3. J. W. Schultz, J. S. Ullett, and R. P. Chartoff, "Novel Liquid Crystal Resins for Stereolithography - Mechanical Properties," *Proceedings of the 8th Solid Freeform Fabrication Symposium*, August 11 - 13, 1997, Austin, Texas.
  4. J. S. Ullett, J. W. Schultz, and R. P. Chartoff, "Novel Liquid Crystal Resins for Stereolithography - Processing Parameters," *Proceeding of the 6th European Conference on Rapid Prototyping and Manufacturing*, July 1- 3, 1997, Nottingham, England.
  5. N. E. Dowling, *Mechanical Behavior of Materials*, Prentice Hall, New Jersey, 1993.
  6. D. J. Broer and G. N. Mol, "Anisotropic Thermal Expansion of Densely Cross-Linked Oriented Polymer Networks," *Poly Eng. & Sci.*, 31, 625 (1991).
  7. J.S. Ullett, J.W. Schultz, and R.P. Chartoff, "Advanced High Temperature Resins for Stereolithography," *Proceedings of the Seventh International Conference on Rapid Prototyping* March 31 - April 3, 1997, San Francisco, CA, p. 203.
  8. P. F. Jacobs, *Rapid Prototyping & Manufacturing Fundamentals of Stereolithography*, McGraw Hill, New York, p. 211 (1992).
  9. R. J. Kar, *Composite Failure Analysis Handbook Vol II: Technical Handbook, Part 2: Atlas of Fractographs*, Final Report, WL-TR-91-4021 (1991).
  10. Xu, Y., Imamura, M., and Nakagawa, T., (1997) " Microscopic Flow Observation of Photopolymer by UV-Laser Exposure," *Proceedings from the 1997 Solid Freeform Fabrication Symposium*, Austin, TX, April 11 - 13, pp 177-184.
- Figure 2

